

1 **Measurements of light absorbing particles on the glaciers**
2 **in the Cordillera Blanca, Peru**

3

4 **C. G. Schmitt^{1,2}, J. D. All^{3,2}, J. P. Schwarz^{4,5}, W. P. Arnott⁶, R. J. Cole^{7,2,*}, E.**
5 **Lapham², A. Celestian³**

6 [1]{National Center for Atmospheric Research, Boulder, Colorado, USA}

7 [2]{American Climber Science Program, Eldora, Colorado, USA}

8 [3]{Western Kentucky University, Bowling Green, Kentucky, USA}

9 [4]{Chemical Sciences Division, Earth System Research Laboratory, National Oceanic and
10 Atmospheric Administration, Boulder, Colorado, USA}

11 [5]{Cooperative Institute for Research in Environmental Sciences, University of Colorado,
12 Boulder, Colorado, USA}

13 [6]{University of Nevada, Reno, Nevada, USA}

14 [7]{Institute of Arctic and Alpine Research, University of Colorado, Boulder, Colorado,
15 USA}

16 [*]{now at: University of Hawaii, Manoa, Hawaii, USA}

17 Correspondence to: C. G. Schmitt (schmittc@ucar.edu)

18

19 **Abstract**

20 Glaciers in the tropical Andes have been rapidly losing mass since the 1970s. In addition to
21 the documented increase in temperature, increases in light absorbing particles deposited on
22 glaciers could be contributing to the observed glacier loss. Here we report on measurements
23 of light absorbing particles sampled from glaciers during three surveys in the Cordillera
24 Blanca Mountains in Peru. During three research expeditions in the dry seasons (May-
25 August) of 2011, 2012 and 2013, two hundred and forty snow samples were collected from
26 fifteen mountain peaks over altitudes ranging from 4800 to nearly 6800 meters. Several
27 mountains were sampled each of the three years and some mountains were sampled multiple
28 times during the same year. Collected snow samples were melted and filtered in the field then

1 later analysed using the Light Absorption Heating Method (LAHM), a new technique that
2 measures the ability of particles on filters to absorb visible light. LAHM results have been
3 calibrated using filters with known amounts of fullerene soot, a common industrial surrogate
4 for black carbon (BC). As sample filters often contain dust in addition to BC, results are
5 presented in terms of effective Black Carbon (eBC). During the 2013 survey, snow samples
6 were collected and kept frozen for analysis with a Single Particle Soot Photometer (SP2).
7 Calculated eBC mass from the LAHM analysis and the SP2 refractory Black Carbon (rBC)
8 results were well correlated ($r^2 = 0.92$). These results indicate that a substantial portion of the
9 light absorbing particles in the more polluted regions were likely BC. The three years of data
10 show that glaciers in the Cordillera Blanca Mountains close to human population centers have
11 substantially higher levels of eBC (as high as 70 ng/g) than remote glaciers (as low as 2.0
12 ng/g eBC), indicating that population centers can influence local glaciers by sourcing BC.

13

14 **1 Introduction**

15 A substantial portion of the population of South America lives on the west coast, where the
16 water supply is supported by the runoff from glacier melt (Barnett et al., 2005). When a
17 region with glaciers is experiencing warming the water availability for the region will change
18 even if precipitation patterns remain constant. Initially, runoff from glaciers will increase as
19 melting increases, but eventually the glacier area will be sufficiently reduced so that the
20 increased melting rate will be offset by the decreased glacier area available for melting and
21 increased water loss due to evaporation, sublimation, or absorption into ground surfaces.
22 Thus, over time the typical water discharge increases as warming starts, reaches a peak, then
23 reduces until a new steady state is reached, presumably after the climate has stopped changing
24 or after the glaciers have completely melted (Baraer et al., 2012). Post warming water flow
25 rates are expected to be significantly below pre-warming flow rates. If glacier melt becomes
26 insignificant, surface water flow rates are then driven more by precipitation, and as a result,
27 dry season water flows can be substantially reduced while wet season flows may not be as
28 significantly impacted. Baraer et al. (2012) estimated the evolution of water flow rates for the
29 Cordillera Blanca region. Their results show that most valleys are past their highest levels of
30 runoff, implying diminishing water supplies into the future if melting persists. The effect of
31 increased BC and dust on this glacial “lifecycle” is to accelerate the process. Increased BC

1 and dust will lead to faster glacier recession, though it is unclear what the effect on runoff
2 would be during the transition phase.

3 In our warming climate, glaciers are melting at a fast rate and tropical glaciers are being
4 substantially impacted. Glaciers in Peru account for more than 70% of the world's tropical
5 glacial area (Kaser, 1999). Rabatel et al. (2013) showed that glaciers in the tropical Andes
6 have receded in area approximately 30% since the 1970s and that areal loss rates have
7 increased substantially in the first decade of the new millennium. Vuille et al. (2008) showed
8 that surface air temperature has increased by 0.10 °C per decade over the last 70 years in the
9 tropical Andes based on measurements from 279 stations between 1°N and 23°S. Similar
10 trends have been shown to exist in studies focusing on temperature evolution in the last
11 several decades from National Centers for Environmental Prediction / National Center for
12 Atmospheric Research (NCEP/NCAR) climate reanalysis data (Kalnay et al., 1996, Bradley et
13 al., 2009). Mark and Seltzer, (2003) used NCEP/NCAR reanalysis data to show that the
14 freezing elevation in the Cordillera Blanca, the location of this study, has risen approximately
15 200 m between 1955 and 2003. Using climate models, Bradley et al. (2006) have shown that
16 tropical glacial regions (above 5000 meters) could experience 4° to 5 °C of temperature
17 increase between 2000 and 2100.

18 In addition to air temperature changes, dust and BC deposited on snow could potentially be a
19 major factor leading to glacial mass loss. BC and dust reduce snow's albedo by absorbing
20 solar radiation, which leads to increased melt and sublimation rates (Warren and Wiscombe,
21 1980). It has recently been shown by Painter et al. (2013) that BC likely led to the end of the
22 little ice age in the European Alps in the mid-1800s. Dust on snow in Colorado has led to
23 substantially increased melt rates (Painter et al., 2012) and has decreased total runoff (Painter
24 et al., 2010). The effects of BC on snow in the Northern Hemisphere has been subject to
25 intensive study, however, despite the fact that glaciers are a critical water source for large
26 populations in South America, no studies to date have measured BC and dust in this region.

27 The Cordillera Blanca range is located in north central Peru. The mountain range is home to
28 17 peaks over 6000 meters and hundreds over 5000 meters. The bulk of precipitation comes
29 from the Amazon basin in the wet season which generally runs from October until May.
30 During the dry season, the atmospheric flows generally come from the west and include more
31 dry air. The dry season in the Cordillera Blanca is not completely dry as it is possible for
32 small storms to pass through the range typically on a weekly basis. These dry season storms

1 can produce snow from a few centimeters to a few tens of centimeters which can sometimes
2 obscure the expected variability of light absorbing particles by depth. Schauwecker et al.
3 (2014) estimated that for the Cordillera Blanca region, there has been a modest temperature
4 increase as well as a modest (60mm/decade) increase in precipitation since the early 1980s.
5 They state that recent changes in temperature and precipitation alone may not explain the
6 glacial recession observed in the 30 years ending in 2012.

7 Sources of BC and dust in the Cordillera Blanca are numerous. Obvious anthropogenic
8 sources of BC include industry and transportation (especially from diesel fuelled vehicles).
9 Industrial sources are mostly centered in and around Huaraz, the largest city (population:
10 100,000, altitude: 3052 meters altitude) abutting the Cordillera Blanca. Regional emission
11 inventories for BC are not available and emission inventories developed for global models are
12 generally based on national emission statistics and do not contain regional specifics. There is
13 substantial agriculture in the Cordillera Blanca region and BC from agricultural burning as
14 well as dust from land clearing and livestock grazing could impact the Cordillera Blanca
15 cryosphere as well. Another potential source of BC is forest clearing and biomass burning in
16 the Amazon basin. Amazonian burning has been estimated to account for approximately 50%
17 of the carbonaceous aerosols in the amazon region (Lamarque et al. 2010, Kaiser et al. 2012).
18 Hydroelectric power is one of the most common forms of energy production and coal burning
19 isn't significant in South America. Increases in dust can be caused by agriculture,
20 construction, mining, and increased traffic on dirt roads.

21 The measurements described in this publication were collected by scientists and volunteers
22 participating in American Climber Science Program (ACSP) expeditions
23 (www.climberscience.com). The ACSP is a research organization with the goal of facilitating
24 research and educational opportunities for scientists and students in regions that are
25 challenging to access. To achieve these goals, experienced climbers are often included in
26 research expeditions in order to increase safety in the mountains. The ACSP research
27 expeditions are also designed to provide opportunities for non-scientists to learn about
28 scientific practices as well as to instruct future scientists on safety in mountain regions. More
29 than fifty international and Peruvian scientists, students, teachers and volunteers have
30 participated in the three ACSP Peru expeditions.

31 Here, we report on three years of measurements of light absorbing particles sampled on
32 glaciers in the Cordillera Blanca. Section 2 describes the field campaigns and the sample

1 collection methods. Section 3 describes a newly developed technique for the quantification of
2 light absorbing particles collected on filters. Section 4 presents the results from the three
3 years of measurements, and the final section discusses the main conclusions of the project.

4

5 **2 Field measurements**

6 The ACSP has conducted three research expeditions during the dry season (austral winter) to
7 the Cordillera Blanca region of Peru beginning in 2011. The sampling of snow and ice for
8 light absorbing particles has been a primary research project during the three expeditions.
9 During the three expeditions, 48, 100, and 90 samples were collected respectively. Samples
10 were taken from glacial surfaces from a minimum altitude of 4800 meters and then at regular
11 altitude intervals to the mountain top. Several mountains were sampled during all three
12 expeditions, and some mountains have been sampled more than once during a single
13 expedition. On one occasion multiple samples were taken at different depths by collecting ice
14 from the walls of a crevasse; these data are used to identify long-term trends in particle
15 loadings.

16 When working in remote and demanding conditions it is important to use simple techniques
17 that provide robust scientific results. Several techniques for snow particle sampling were
18 considered before a filtering technique was chosen. The technique for sampling particles in
19 snow is similar to the technique used by the University of Washington's "Soot in Arctic
20 Snow" group (as described in Doherty et al. 2010).

21 During research expeditions, volunteer scientists collect snow samples from pre-determined
22 locations on each mountain. Samples are collected from approximately 100 meters above the
23 snow line to the summit at 200 to 500 vertical meter intervals, the exact interval depends on
24 the height of the mountain and the complexity of the terrain. Volunteers are instructed to
25 avoid areas near exposed rock as well to areas that may be near avalanche paths or could be
26 affected by debris from avalanches. Because mountain climbing is a physically demanding
27 and potentially dangerous activity, the ultimate decisions on how high and where to collect
28 samples is left to the discretion of the climbing team with safety being the highest priority.
29 Global Positioning System way points are taken and, if possible, samples are collected from
30 the same location as on previous climbs. Snow samples were collected by scooping snow into
31 four liter ziplock plastic bags. Bags are labelled on the outside with a permanent marker after
32 the bag has been sealed. Typically, ACSP volunteers collected samples with hands that had

1 been ‘contaminated’ with local snow. This is done by washing hands with snow so that any
2 contaminants on the hands are similar to those in the snow. Since snow is collected on the
3 descent usually well after sunrise, the snow is soft enough that it is easy to fill a bag
4 contacting the snow only minimally. For each sample approximately 1 kilogram of snow is
5 collected at each site from both the surface (defined as the top 2.5 cm) and the sub-surface
6 (deeper than 2.5 cm). The idea was that the surface sample should give an indication of any
7 dry deposition that has occurred since the last snow storm as well as any accumulation of
8 contaminants on the surface due to melting and sublimation while the sub-surface samples
9 should contain any contaminants that came with the most recent snowstorm either as ice
10 nuclei or as having been scavenged by falling snow. In reality, it was commonly found that
11 fresh snowfall during the dry season amounted to less than 10 cm. The result was that the
12 sub-surface sample often contained snow that had been subject to dry deposition and surface
13 accumulation before the most recent snowfall. Once samples were collected and labelled, the
14 snow samples are packed together into backpacks and returned to basecamp for processing.

15 In camp, snow samples are melted one at a time by placing the ziplock bags in warm water
16 (usually around 30°C). Once melted, snow-sourced water is drawn into 60 mL syringes and
17 pumped slowly through 0.7 micron “Pallflex tissuquartz” type 25 mm quartz fiber filters. A
18 total of 600mL of snow-water is filtered per sample unless the filter becomes too clogged in
19 which case less water is filtered and the amount of filtered water is recorded. The samples are
20 filtered immediately after melting to minimize adhesion of particles to the surface of the bag.
21 The typical time between the starting of melting and the completion of filtering is 15 to 20
22 minutes. Filters are removed from filter holders, placed into plastic capsules designed for
23 coin collections, and held in place with a thin foam ring. After each field excursion, filters are
24 returned to Huaraz where they are dried in the sun, then stored in a freezer until the end of the
25 expedition when they are returned to the US for analysis.

26

27 **3 Filter Analysis**

28 A new technique has been developed for the analysing the light absorption properties of
29 particles collected on filters. The Light Absorption Heating Method (LAHM) is a cost
30 effective technique that can be used to accurately quantify the impact of light absorbing
31 particles on snow. The premise behind conducting measurements of light absorbing particles
32 in snow is to estimate the amount of light energy the particles will absorb leading to increased

1 melting or sublimation. Because snow is completely absorptive in the thermal infrared
2 wavelength range, the more critical wavelengths to consider are in the visible range.
3 Understanding the absorption of solar radiation in the visible wavelength range by particles in
4 snow is the goal of the research. The LAHM analysis technique described here approaches
5 the problem directly by measuring the temperature increase of a particle load on a filter when
6 visible light is applied. A diagram of the LAHM setup is shown in Fig. 1. Each filter is
7 suspended on plastic wrap a few centimetres above a pool of cool water. Water is used
8 because it provided a thermally stable background compared to a solid surface which could
9 absorb visible radiation. Plastic wrap does not absorb visible light and as such it provides a
10 neutral background and is of low mass per unit area thus having a negligible effect on
11 measurements. An infrared thermometer (IR thermometer: Omega OS1327D) which can
12 record data every second is mounted above the filter to measure the temperature of the filter
13 without touching it. To determine the light absorption ability of the materials, a laboratory
14 grade light source (Cole-Parmer Fiber-Lite Fiber Optical Illuminator Model 9745-00) with a
15 fiber optic light pipe to direct the light is mounted close to the filter and shines light at
16 approximately a 45° angle to the filter (thus reducing the effects of multiple reflections in the
17 system). The light transmitted through the light pipe only spans the visible wavelengths from
18 300-800 nm. The particles on the filter absorb light causing the filter to warm. The IR
19 thermometer records the temperature of the filter every second and data are saved to a
20 computer for later analysis. After an initial ten seconds to establish a base temperature, the
21 light source is turned on for 30 seconds, then extinguished while the temperature of the filter
22 is recorded for an additional 50 seconds. Temperature increases are normalized by the
23 average temperature recorded during the first ten seconds. The maximum temperature
24 increase of a filter ranges from less than 1°C for a clean filter, up to 10°C for the most heavily
25 contaminated filters. During analysis, after every ten filters, two control filters were tested to
26 assure consistency in the setup. The control filters included an unused clean filter and a
27 calibration filter with a heavy load of BC. Sample temperature profiles from 8 filters
28 collected during the 2011 expedition are shown in Fig. 2.

29 The LAHM analysis technique was calibrated by sampling a BC standard: water with a
30 known concentration of BC (Schwarz et al., 2012). The BC standard has 10% uncertainty.
31 Filters with low and high BC loads were made by filtering different amounts of BC standard.
32 The BC standard was made with fullerene soot, a reference material used in the single-particle
33 BC detection community (Baumgardner et al., 2012). The filters used for calibration

1 (Millipore mixed cellulose ester filter membrane 0.22 micron) are different from the filters
2 that have been used in the field (Pallflex Membrane tissuquartz 0.7 micron). The BC standard
3 was created with BC particles in the size range generally found in the atmosphere (0.2 to 0.8
4 microns) which were not captured well by the tissuquartz filters. Torres et al. (2014) found
5 that tissuquartz filters captured less than 38% of the BC mass when filtering rainwater. The
6 mass size distribution for their measurements peaked between 210 and 240 nm, similar to
7 atmospheric BC sizes but smaller than the peak sizes expected in snow (Schwarz et al. 2012).
8 The tissuquartz filters are used in the field because water flow through the filters is much
9 faster making them much easier to use in the field and the filter material enables additional
10 types of analysis that are not possible with the Millipore filters. Temperature profiles
11 recorded for unused filters of both types were nearly identical (well within the SD of
12 measurements), indicating that the filter type did not bias the temperature measurement
13 technique significantly. Three calibration filters at each of four different fullerene soot mass
14 amounts (5-20 micrograms) were created as well as one calibration filter with 30.0
15 micrograms. The temperature increase for each calibration filter was determined at least four
16 times and the overall standard deviation in the temperature increase at each carbon level was
17 used in the uncertainty determination. Figure 3 shows plots of twelve temperature increase
18 profiles measured for the three calibration filters loaded with 10 micrograms of fullerene soot.
19 The mean values and standard deviations are also shown, along with a calibration curve
20 showing the relationship between BC mass and heating after ten seconds. Standard deviation
21 values were generally less than 0.5 °C and remained constant throughout the heating phase.
22 Note that the heating for blank filters was approximately 0.6 °C on average, just above the SD
23 for the shown measurements. Several of the cleanest filters from mountain samples from
24 each year had temperature increases of less than 1.0 °C.

25 Laboratory measurements of post-filtered samples showed that the tissuquartz filters did not
26 efficiently collect BC particles smaller than about 0.6 microns. In the atmosphere most BC
27 mass is distributed across particles smaller than this, but BC in snow has been shown to exist,
28 in some samples, at sizes up to a few microns (Schwarz et al., 2012). While it is clear that the
29 tissuquartz filters may not be collecting all of the BC, it is unclear what portion is being
30 missed. Results of separate mineralogy tests suggest that there were high concentrations of
31 dust which can clog the pores and anecdotal evidence (volunteers noting that it had become
32 very difficult to push the water through the filters) suggests that the effective pore size
33 substantially decreases as dusty samples are being filtered. Given that BC particles in this size

1 range can be missed, the BC on the sample filters is likely an underestimate of the true BC in
2 the snow. Since this under-catch was noticed, tests have been conducted using snow from
3 tropical glaciers that indicate that the missed particles do not account for much absorption.
4 Snow sourced water that had already been passed through a tissuquartz filter was collected
5 and passed through a 0.22 micron filter. While the tissuquartz filters in these tests captured
6 high concentrations of particles, the 0.22 micron filters appeared clean after filtering and
7 results from the LAHM technique were below the detection threshold. Of the approximately
8 20 tests filters, the eBC value estimated for the 0.22 micron filter was never more than 20% of
9 the value determined for the tissuquartz filter and the average was around 5%, well within the
10 noise level of the LAHM technique at these levels.

11 The LAHM technique doesn't discriminate between BC and dust. Therefore, the values
12 derived from the LAHM technique should be treated as "effective black carbon" (eBC)
13 meaning that the visible light absorptive capacity of the particles on the sample filter are
14 equivalent to the given amount of BC (Grenfell et al., 2011).

15 The increase in temperature of the calibration filters after ten seconds of exposure to light was
16 used to derive a fit equation to predict the mass of BC on the calibration filters. The r^2 value
17 of the fit equation was 0.98 with an uncertainty of approximately $\pm 20\%$ (10% from the BC
18 standard and 10% for the typical SD calculated and shown in Fig. 3b). This uncertainty likely
19 increases with higher filter loads given that the temperature response to BC curve flattens
20 (Fig. 3c). On heavily loaded filters, this flattening could be due to some of the BC being
21 hidden under other layers of particles and therefore not absorbing as much light energy as
22 other BC on the filter. It was found, however, that filter samples collected in the field often
23 had different slopes to their temperature increase, particularly after 20 s of illumination. It is
24 suspected that this is due to dust mixed in with the BC changing the overall heat capacity.
25 Figure 4 shows two temperature profiles, one from a fullerene soot calibration filter and one
26 from a sample filter suspected to contain significant dust as well as a substantial amount of
27 BC. Note that the temperature curves are nearly identical for approximately ten seconds after
28 illuminating the lamp before they begin to diverge. It is thought that dust mixed in with BC
29 on a filter could be causing this divergence. Filters collected in other regions with
30 substantially higher dust concentrations and low BC concentrations showed much steeper
31 temperature increases later in the heating phase. This would suggest that the effects of BC

1 and dust could be separated with the LAHM technique, but quantification of this is beyond
2 the scope of this publication.

3 Data from 2011 were collected with a slightly different filtering setup than subsequent
4 expeditions. The change was made because the type of filter housing used in 2011
5 occasionally came into contact with the surface of the filter leading to the removal of some of
6 the particles when the filter housing was opened. We estimate that this may have reduced the
7 filter loading by up to 25%. This estimate is based on the approximate area of the filter that
8 appeared to be scraped clean as well as the fact that the filter holder had obvious particle
9 loading that corresponded to the cleaned area. While it is not possible to determine the exact
10 amount of material lost, the eBC values estimated for the affected filters were multiplied by
11 1.25.

12 During the 2013 expedition, 12 unmelted snow samples were collected in acid washed glass
13 vials and returned to the US for analysis with a Single Particle Soot Photometer (SP2)
14 instrument (see Schwarz et al., 2012). These samples were collected from two mountains:
15 one in a region suspected to be highly polluted due to its proximity to Huaraz and another
16 mountain in a more remote region. Additional snow samples were collected for filtering from
17 the same locations for comparison. Results from the LAHM technique are compared to SP2
18 refractory Black Carbon (rBC; Baumgardner et al. 2012) mass concentration measurements in
19 Fig. 5. Note that while there is some variability between the techniques, the results are
20 reasonably correlated ($r^2 = 0.92$). Microscale variability could have accounted for some of the
21 differences. Figure 5 shows that for some of the comparisons, the SP2 rBC values were higher
22 than the LAHM eBC values. This could be due to non-uniformity in snow as the LAHM
23 technique uses much more snow than the SP2 (600 g for LAHM vs. ~ 10 g for SP2).
24 Additionally, the tissuquartz filter could have missed a fair amount of the BC mass due to the
25 large pore size.

26

27 **4 Results**

28 The eBC values determined by the LAHM technique for all measurements collected during
29 the three expeditions are shown in Fig. 6 plotted by altitude. Values of eBC range from the
30 quite low: 2.0 ng-eBC/g-H₂O up to almost 80 ng/g. The highest altitudes have substantially
31 less eBC while lower altitude values were larger; although numerous measurements still show
32 values of less than 10.0 ng/g eBC at low altitudes. The largest values are similar to those

1 reported by Ye et al. (2012) who reported values between 20 and 70 ng/g of BC in
2 northwestern China seasonal snow at altitudes up to 3500 meters. Huang et al. (2011)
3 measured much larger values (over 1000ng/g) of eBC in northeastern China, where dust was
4 common as well as high levels of BC. The Cordillera Blanca measurements of eBC compare
5 similarly in value and variability to those observed by Doherty et al. (2013) in Alaska and
6 Greenland and are similar to those reported by Grenfell et al. (1981) for the Washington
7 Cascade mountains (22-59 ng/g). The values are somewhat lower than those reported by
8 Sergent et al. (1993) for the French Alps (80-280 ng/g).

9 **4.1 Surface accumulation**

10 As stated in the field measurements section, it was rare to collect samples where the surface
11 sample contained long term dry deposition and surface accumulation and the sub-surface
12 sample contained only pristine snow. Often, the snow from the previous storm had
13 compacted enough that the sub-surface sample contained snow that had been previously
14 exposed as a surface. This led to the eBC values for the surface and sub-surface samples to
15 not be consistently related. During the three expeditions there were 92 paired measurements
16 where a surface sample and a sub-surface sample were collected. Of those samples, in 56
17 cases, the surface sample contained higher eBC values than the sub-surface samples while for
18 the remaining 36 samples the opposite was true. The average ratio (averaged in log-space)
19 was 0.96 suggesting that on the average, the surface and sub-surface samples were
20 statistically similar. The average difference between the two samples was a factor of 2.17
21 with a maximum difference of a factor of 12. Based on the fact that it does snow from time to
22 time in the dry season, and that samples are never collected near the zone of ablation, the
23 differences are thought to be due to short term changes in the snow pack rather than annual
24 variability. Figure 7 shows a probability distribution function of the ratio between the surface
25 measurement to the sub-surface measurement for the 92 pairs of measurements.

26 **4.2 By Region**

27 Fig. 8 shows a map of the Cordillera Blanca region and the eBC values in snow determined
28 from filter samples using the LAHM analysis technique for filter samples collected in
29 different areas during each of the three expeditions. For the three expeditions, the data are
30 grouped into five different valleys or mountains that were sampled each of the three years.
31 Regions 1 and 2 lie on the north end of the range and consist of the mountains in the Santa

1 Cruz and Paron valleys (region 1, 70 km from Huaraz), and Llanganuco valley (region 2, 54
2 km from Huaraz). These regions are characterized by higher precipitation and lower nearby
3 population densities. The mountains around Ishinca valley (region 3, 21 km from Huaraz),
4 Vallunaraju mountain (region 4, 14 km from Huaraz), and the mountains around the
5 Quilcayhuanca valley (region 5, 24 km from Huaraz) are all clustered near Huaraz, the largest
6 population center in the region. The eBC values shown in Fig. 8 are determined by taking an
7 average of all measurements of surface and sub-surface snow in each of the regions. As the
8 relationship between the surface and sub-surface values was highly variable (as shown in Fig.
9 7), the averaged values are thought to better represent the typical conditions for the top 10 cm
10 of snow. Standard deviations of the measurements in each region are shown in Fig. 8. Data
11 from all three years show a distinct trend, with the southern regions having 2-3 times more
12 light absorbing particles compared to the northern regions. The SP2 measurements discussed
13 in the calibration section were collected in 2013 in region 2 and 4. The region 2 SP2
14 measurements averaged a 0.65 ng/g while the region 4 SP2 values averaged 31.0 ng/g. The
15 LAHM technique suggests that the eBC values in region 1 and 2 would be on the order of 10
16 ng/g while the SP2 rBC was much lower. This leads us to the hypothesis that the bulk of the
17 temperature increase on the filters from region 1 and 2 is likely due almost exclusively to dust
18 rather than BC, while in regions 3-5, near the city of Huaraz, BC likely makes up a substantial
19 portion of the absorptive particle matter present on the filters because the eBC values and the
20 SP2 rBC values are similar in magnitude in region 4. Differences observed from year to year
21 in each region are likely due to sampling being weighted to different altitudes or mountains
22 rather than substantial changes in pollutant levels.

23 Fig. 9 shows the mean value and standard deviation for data collected from all three years
24 separated by altitude. Data are binned into two groups: region 1 and 2 in one group and 3-5 in
25 the second group for all three years combined. Note the relatively linear decrease in eBC with
26 altitude for both regions. Thin lines show the standard deviation calculated for the more
27 numerous measurements. In general, eBC concentration levels decrease with altitude, though
28 it should be noted that there are few measurements at altitudes above 6000 meters and those
29 are mostly in region 2.

30 **4.3 By Depth**

31 During the 2012 expedition, samples were collected from the wall of a newly opened crevasse
32 on Vallunaraju mountain in region 4. Vallunaraju is the nearest glaciated mountain to Huaraz

1 and has some of the highest eBC measurements using the LAHM technique as well as the
2 highest concentration observed by the SP2 (75 ng-rBC/g-H₂O). Fig. 10 shows the eBC
3 values for the samples collected from the crevasse wall as a function of depth in the crevasse.
4 There were several dark streaks at relatively uniform spacing down the crevasse wall which
5 are suspected to be surface accumulations during the dry seasons (local glaciology experts
6 agreed with this assessment). The eBC measurements higher than 20 ng/g in Fig. 10 were
7 from the darker areas while the lower values were from cleaner ice that dominated the
8 crevasse wall. It is suspected that the cleaner samples were from wet season storms. A
9 distinct decrease of eBC values with depth can be seen in the suspected wet season samples.
10 While this might indicate that black carbon values have been increasing in recent wet seasons,
11 the values are low enough that the trend is within the expected uncertainty range.

12

13 **5 Conclusions**

14 It is well documented that tropical glaciers are melting rapidly with concurrent effects on
15 critical water supplies. Numerous factors could be contributing to low latitude glacier mass
16 loss, including larger concentrations of light absorbing particles on glacier surfaces. Because
17 melting glacial water is an important natural resource in the region for agriculture,
18 hydroelectric power, and drinking water, an increased understanding of the pressures on this
19 resource could aid regional planners in adapting to future regional climate changes. This
20 paper presents the results of three years of measurements of light absorbing particles on the
21 glaciers in the Cordillera Blanca in Peru. Samples were collected by volunteers participating
22 in American Climber Science Program expeditions. Snow samples collected from glacier
23 surfaces were melted, and the light absorbing particles collected on filters.

24 A new technique (called the LAHM technique herein) to quantify the amount of visible
25 radiation the light absorbing particles can absorb has been developed and calibrated using
26 filters with a known amount of black carbon. These “effective Black Carbon” estimates from
27 the LAHM technique were found to be well correlated ($r^2 = 0.92$) with refractory black carbon
28 mass measurements made with the Single Particle Soot Photometer 2 instrument for a subset
29 of the measurements. The LAHM technique provides an accurate, useful, and cost effective
30 way to measuring light absorbing particles in snow.

31 In the Cordillera Blanca, the concentration of light absorbing particles was highest near
32 Huaraz, the largest city in the region, while samples from more remote regions contained

1 substantially lower amounts of absorptive material. The measured levels of light absorbing
2 particles in the snow near Huaraz absorb a similar amount of visible radiation as snow that
3 contains between 20 to 80 ng/g of black carbon. This amount of black carbon in pristine fresh
4 snow can result in a decrease in spectral albedo of greater than 1% (SNICAR – online,
5 Flanner et al., 2007).

6

7 **Acknowledgements**

8 This work would not have been possible without the help of the American Climber Science
9 Program volunteers for the 2011, 2012, and 2013 expeditions. The authors specifically wish
10 to thank Frank Nederhand for initiating the program that would lead to the ACSP and Chris
11 Benway at La Cima Logistics in Huaraz, Peru for helping to organize the expeditions.
12 Thanks to Darrel Baumgardner for helping to facilitate the SP2 measurements as well as for
13 helping to bring this work to the attention of the Pollution and its Impacts on the South
14 American Cryosphere (PISAC) Initiative. Thanks to Karl Froyd and Jin Liao for their helpful
15 comments and analysis with the PALMS instrument. Thanks also to Huascarán National
16 Park, Jesus Gomez park director, for helping ensure the long term success of this research.
17 Additional thanks go to the many generous donors who have made the ACSP expeditions
18 possible. Also, the American Alpine Club whose early assistance was invaluable.

19

1 **References**

- 2 Baraer, M., Mark B. G., McKenzie J. M., Condom, T., Bury, J., Huh, K-I., Portocarrero, C.,
3 and Gomez J.: Glacier recession and water resources in Peru's Cordillera Blanca, J.
4 *Glaciology*, 58, 134-150, doi:10.3189/2012JoG11J186, 2012.
- 5 Barnett, T. P., Adams, J. C., and Lettenmaier, D. P.: Potential impacts of a warming climate
6 on water availability in snow-dominated regions, *Nature*, 438, 303-309,
7 doi:10.1038/nature04141, 2005.
- 8 Baumgardner, D., Popovicheva, O., Allan, J., Bernardoni, V., Cao, J., Cavalli, F., Cozic, J.,
9 Diapouli, E., Eleftheriadis, K., Genberg, P. J., Gonzalez, C., Gysel, M., John, A., Kirchstetter,
10 T. W., Kuhlbusch, T. A. J., Laborde, M., Lack, D., Muller, T., Niessner, R., Petzold, A.,
11 Piazzalunga, A., Putaud, J. P., Schwarz, J., Scheridan, P., Subramanian, R., Swietlicki, E.,
12 Valli, G., Vecchi, R., and Viana, M.: Soot reference materials for instrument calibration and
13 intercomparisons: a workshop summary with recommendations, *Atmos. Meas. Tech.*, 5,
14 1869-1887, doi:10.5194/amt-5-1869-2012.
- 15 Bradley, R. S., Vuille, M., Diaz, H. F., and Vergara W.: Threats to water supplies in the
16 tropical Andes, *Science*, 312, 1755-1756, DOI: 10.1126/science.1128087, 2006.
- 17 Doherty, S. J., Warren, S. G., Grenfell, T. C., Clarke, A. D., and Brandt, R. E.: Light-
18 absorbing impurities in arctic snow, *Atmos. Chem. Phys.*, 10, 11647-11680, 2010.
- 19 Doherty, S. J., Grenfell, T. C., Forsström, S., Hegg, D. L., Brandt R. E., and Warren S. G.:
20 Observed vertical redistribution of black carbon and other insoluble light-absorbing particles
21 in melting snow, *J. Geophys. Res. Atmos.*, 118, 5553–5569, doi:10.1002/jgrd.50235, 2013.
- 22 Flanner, M. G., Zender, C. S., Randerson J. T., and Rasch P. J.: Present day climate forcing
23 and response from black carbon in snow, *J. Geophys. Res.*, 112, D11202,
24 doi:10.1029/2006JD008003, 2007.
- 25 Grenfell, T. C., Perovich, D. K., and Ogren, J. A.: Spectral albedos of an alpine snowpack,
26 *Cold Reg. Sci. Technol.*, 4, 121–127, 1981.
- 27 Grenfell, T. C., Doherty, S. J., Clarke, A. D., and Warren S. G.: Light absorption from
28 particulate impurities in snow and ice determined by spectrophotometric analysis of filters,
29 *Applied Optics*, 50, 1-12, 2011.

1 Huang, J, Fu, Q., Zhang, W., Wang, X., Zhang, R., Ye, H., and Warren, S. G.: Dust and black
2 carbon in seasonal snow across northern China. *B. Am. Meteorol. Soc.*, 92, 175-181,
3 DOI:10.1175/2010BAMS3064.1, 2011.

4 Kaiser, J., Heil, A., Andreae, M., Benedetti, A., Chubarova, N., Jones, L., Morcrette, J.-J.,
5 Razinger, M., Schultz, M. G., Suttie, M., and van der Werf, G. R.: Biomass burning emissions
6 estimated with a global fire assimilation system based on observed fire radiative power.
7 *Biogeosciences* 9, 527-554, 2012.

8 Kalnay, E., Kanamitsu, M., Kistler, R., Collins, W., Deaven, D., Gandin, L., Iredell, M., Saha,
9 S., White, G., Woollen, J., Zhu, Y., Chelliah, M., Ebisuzaki, W., Higgins, W., Janowiak, J.,
10 Mo, K. C., Ropelewski, C., Wang, J., Leetmaa, A., Reynolds, R., Jenne, R., and Joseph, D.:
11 The NCEP/NCAR 40-year reanalysis project, *B. Am. Meteorol. Soc.*, 77, 437–471, 1996.

12 Kaser, G.: A review of the modern fluctuations of tropical glaciers, *Glob. Planet. Change*, 22,
13 93–103, 1999.

14 Lamarque, J.-F., Bond, T. C., Eyring, V., Granier, C., Heil, A., Klimont, Z., Lee, D., Liousse,
15 C., Mieville, A., Owen, B., Schultz, M. G., Schindell, D., Smith, S. J., Stehfest, E., Van
16 Aardenne, J., Cooper, O. R., Kainuma, M., Mahowald, N., McConnell, J. R., Naik, V.,
17 Riahi, K., van Vuuren, D. P.: Historical (1850–2000) gridded anthropogenic and biomass
18 burning emissions of reactive gases and aerosols: methodology and application. *Atmospheric*
19 *Chemistry and Physics* 10, 7017-7039, 2010.

20 Mark, B. G. and Seltzer, G. O.: Tropical glacier meltwater contribution to stream discharge: a
21 case study in the Cordillera Blanca, Peru, *J. Glaciol.*, 49, 271–281, 2003.

22 Painter, T. H., Deems, J. S., Belnap, J., Hamlet, A. F., Landry, C. C., Udall, B.: Response of
23 Colorado river runoff to dust radiative forcing in snow, *Proceedings of the national academy*
24 *of sciences*, doi/10.1073/pnas.0913139107, 2010.

25 Painter, T. H., Skiles, S. M., Deems, J. S., Bryant, A. C., and Landry, C. C.: Dust radiative
26 forcing in snow of the upper Colorado river basin: 1. A 6 year record of energy balance,
27 radiation, and dust concentrations. *Water Resources Research*, 48, W07521,
28 doi:10.1029/2012WR011985, 2012.

29 Painter, T. H., Flanner, M. G., Kaser, G., Marzeion, B., VanCuren, R. A., and Abdalati, W.:
30 End of the Little Ice Age in the Alps forced by industrial black carbon, *Proceedings of the*
31 *national academy of sciences*, doi: 10.1073/pnas.1302570110, 2013.

1 Rabatel, A., Francou, B., Soruco A., Gomez, J., Caceres, B., Cabellos, J. L., Basantes, R.,
2 Vuille, M., Sicart, J. E., Huggel, C., Scheel, M., Lejeune, Y., Arnaud, Y., Collet, M.,
3 Condom, T., Consoli, G., Favier, V., Jomelli, V., Galarraga, R., Ginot, P., Maisincho, L.,
4 Mendoza, J., Menegoz, M., Ramirez, E., Ribstein, P., Suarez, W., Villacis, M., and Wagnon,
5 P.: Current state of glaciers in the tropical Andes: a multi-century perspective on glacier
6 evolution and climate change. *The Cryosphere*, 7, 81-102, doi:10.5194/tc-7-81-2013.

7 Schauwecker, S., Rohrer, M., Acuna, D., Cochichin, A., Davila, L., Frey, H., Giraldez, C.,
8 Gomez, J., Huggel, C., Jacques-Coper, M., Loarte, E., Salzmann, N., Vuille, M.: Climate
9 trends and glacier retreat in the cordillera blanca, Peru, revisited. *Global and Planetary*
10 *Change*, 119, 85-97, 2014.

11 Schwarz, J. P., Doherty, S. J., Li, F., Ruggiero, S. T., Tanner, C. E., Perring, A. E., Gao, R. S.,
12 and Fahey, D. W.: Assessing Single Particle Soot Photometer and Integrating
13 Sphere/Integrating Sandwich Spectrophotometer measurement techniques for quantifying
14 black carbon concentration in snow, *Atmos. Meas. Tech.*, 5, 2581–2592, doi:10.5194/amt-5-
15 2581-2012.

16 Sergent, C., Pougatch, E., and Sudul, M.: Experimental investigation of optical snow
17 properties, *Ann. Glaciol.*, 17, 281–287, 1993.

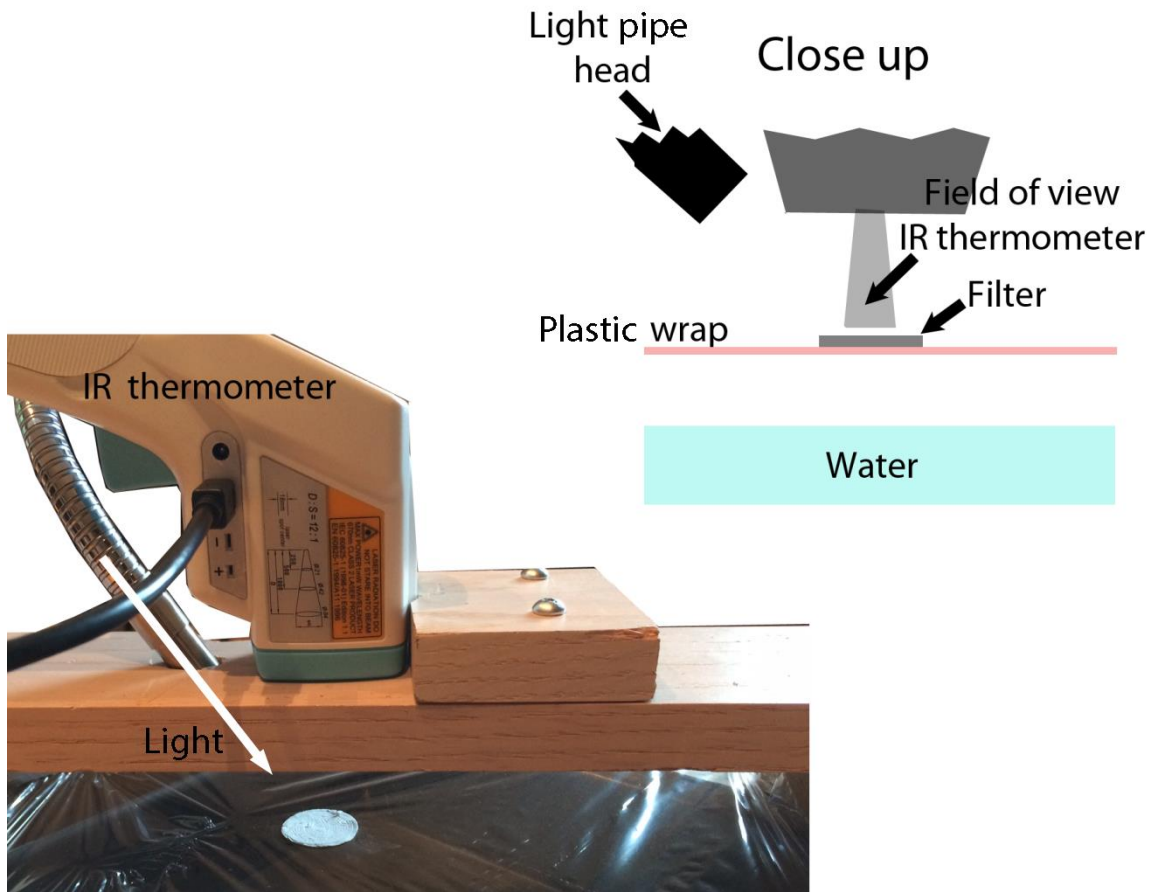
18 Torres, A., Bond, T. C., Lehmann, C. M. B., Subramanian, R., and Hadley, O. L.; Measuring
19 organic carbon and black carbon in rainwater: evaluation of methods, *Aerosol Science and*
20 *Technology*, 48:3, 239-250, DOI: 10.1080/02786826.2013.868596, 2014.

21 Vuille, M., Francou, B., Wagnon, P., Juen, I., Kaser, G., Mark, B. G., and Bradley, R. S.:
22 Climate change and tropical Andean glaciers: past, present and future. *Earth-Science*
23 *Reviews*, 89, 79-96, doi:10.1016/j.earscirev.2008.04.002, 2008.

24 Warren, S. G., and Wiscombe W. J.: A model for the spectral albedo of snow II: Snow
25 containing atmospheric Aerosols, *Journal of the Atmospheric Sciences*. 37, 2734-2745, 1980.

26 Ye, H., Zhang, R., Shi, J., Huang, J., Warren, S. G., and Fu, Q.: Black carbon in seasonal
27 snow across northern Xinjiang in northwestern China. *Environmental Research Letters*, 7, 1-
28 9, doi:10.1088/1748-9326/7/4/044002, 2012.

29

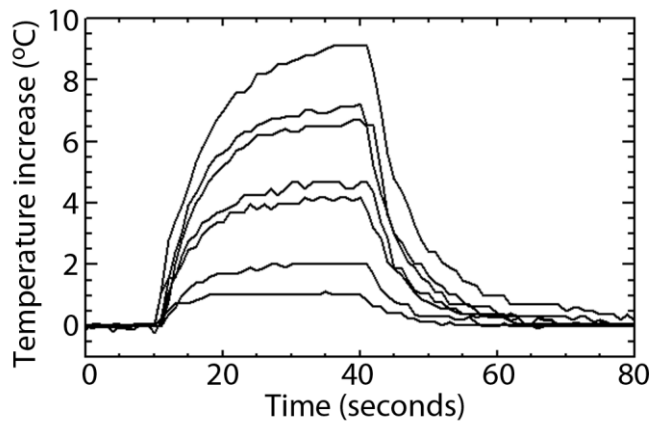


1

2

3 Figure 1. Diagram of the LAHM analysis setup. A light source is aimed at a 45° angle at the
 4 filter which rests on plastic wrap approximately 10 cm above the water surface. The infrared
 5 thermometer directly views the center of the filter. The field of view of the thermometer is
 6 approximately 1.5 cm at the distance of the filter and the contaminant spot on the filter is
 7 generally 2 cm in diameter.

8

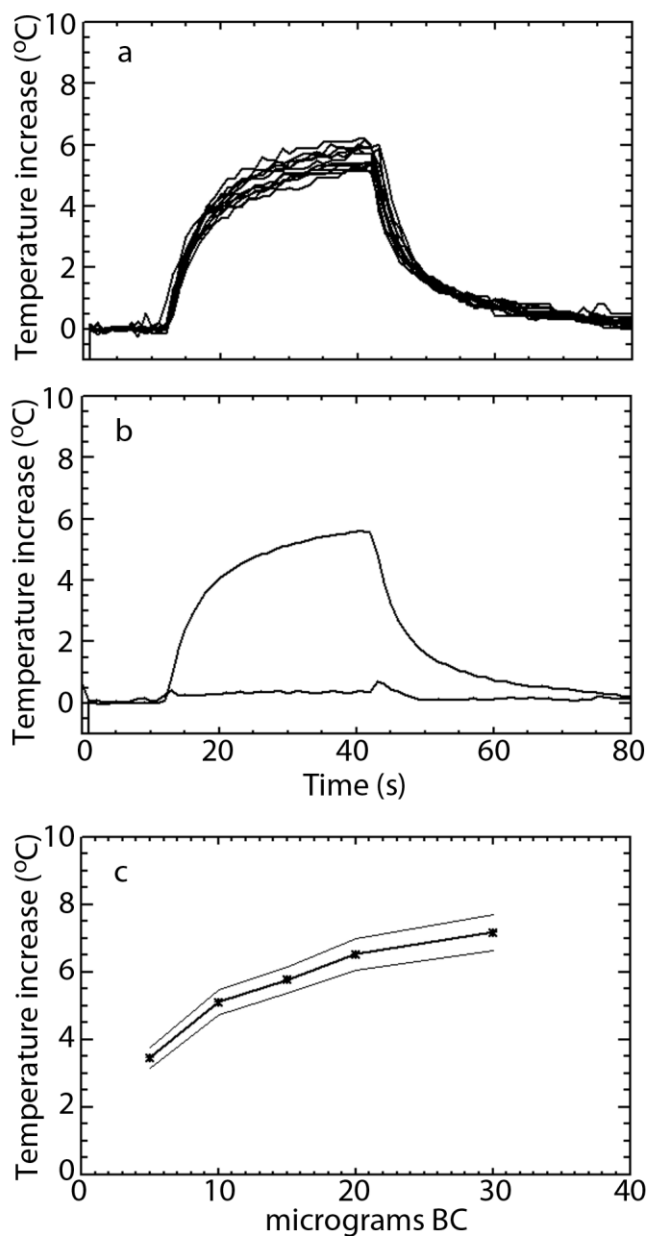


1

2

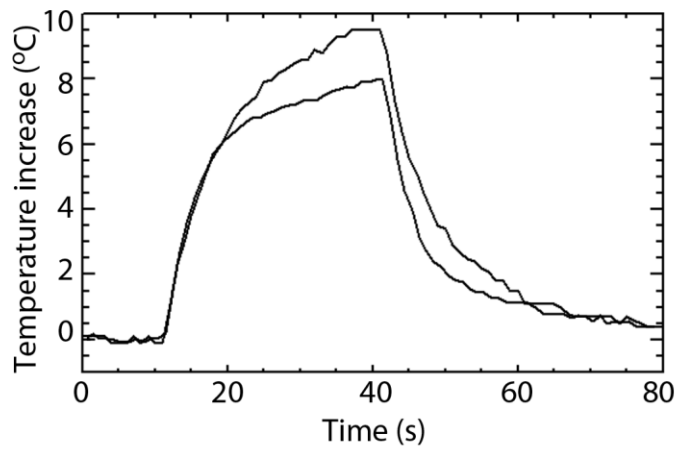
3 Figure 2. Measured temperature profiles for 7 filters with a variety of light absorbing particle
4 loads. Temperature recording started ten seconds before the lamp was illuminated, and the
5 lamp was extinguished 30 seconds later. Temperatures are normalized to the average of first
6 10 seconds of data and the temperature usually returned to the start temperature within a
7 minute of the lamp being extinguished.

8



1
2
3
4
5
6
7
8

Figure 3. a) Twelve temperature profiles measured for filters with 10 micrograms of fullerene soot. Profiles are from three different filters measured four times each. b) Mean temperature profile and standard deviation for 12 temperature profiles shown in 3a. c) Temperature increases after ten seconds for five masses of fullerene soot. Error bars are standard deviations for each measurement and bold line is fit to data.

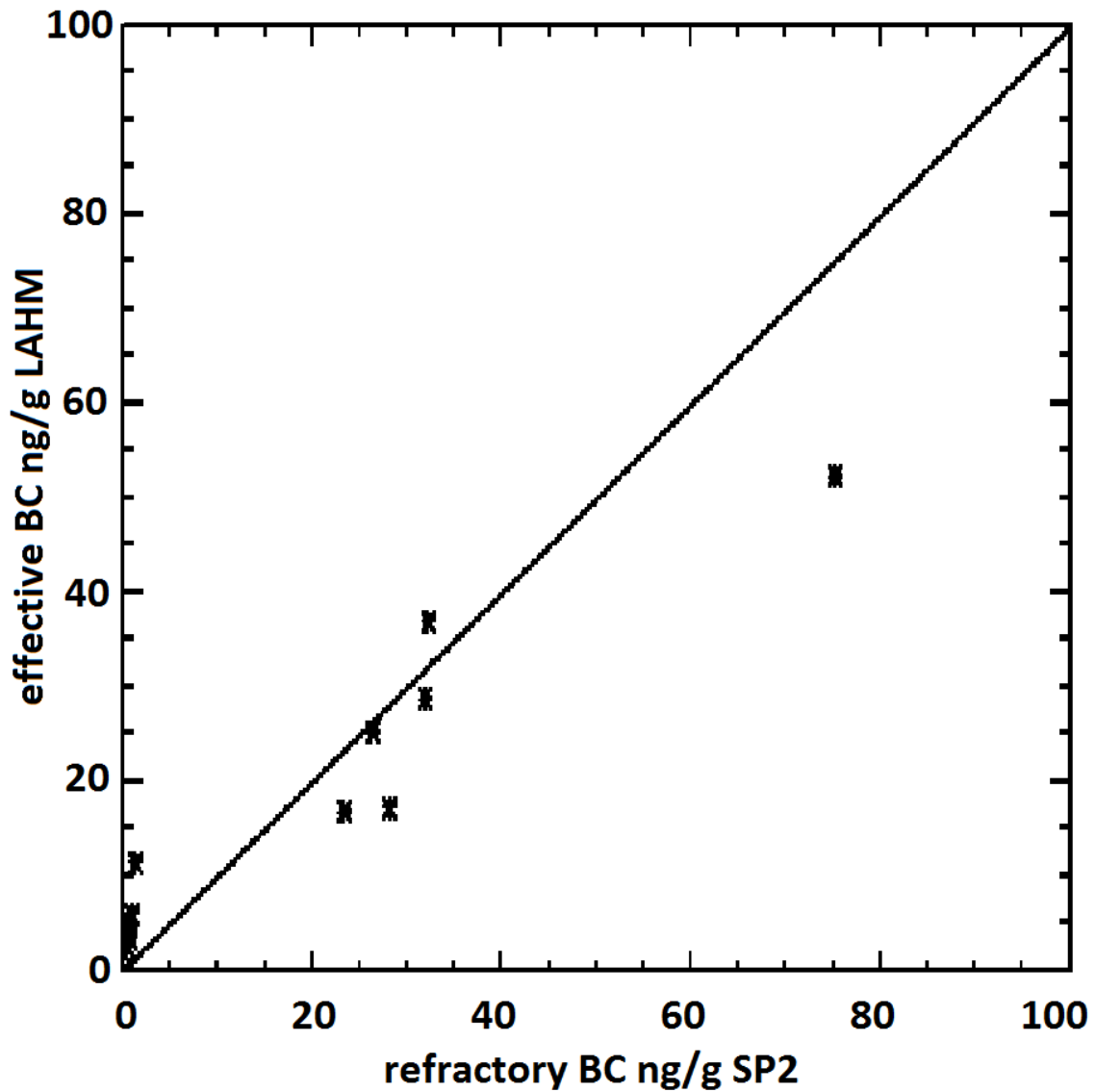


1

2

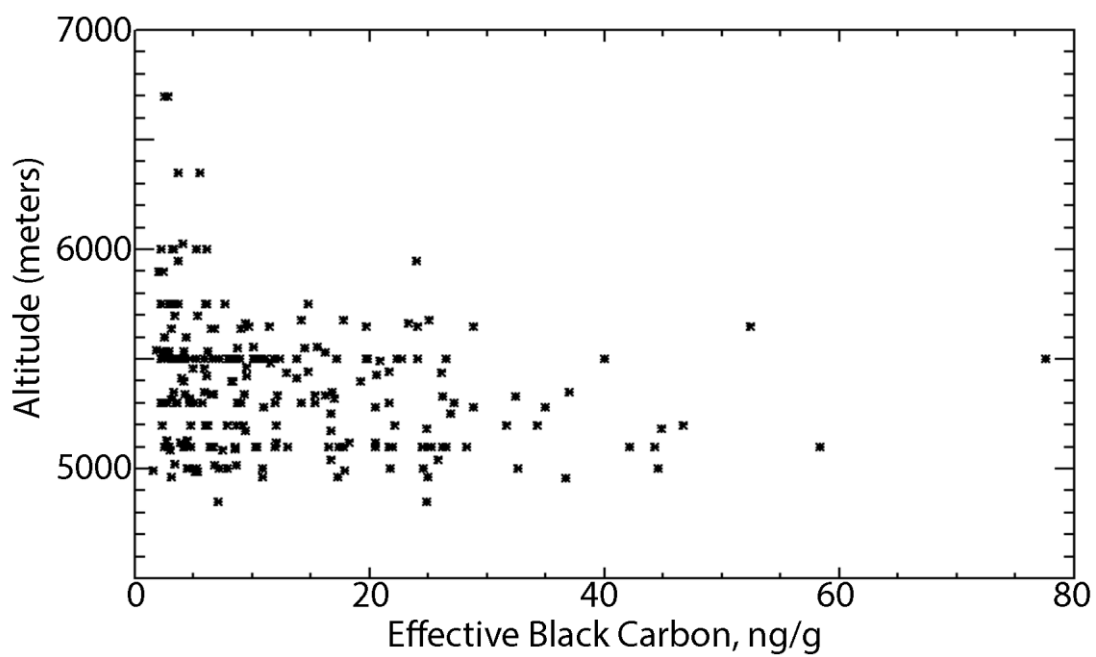
3 Figure 4. Temperature profiles measured for a calibration filter with fullerene soot (lower
4 curve), and a sample filter with dust and black carbon (upper curve). The curves are nearly
5 identical until 20 seconds (10 seconds of heating) after which they diverge. The continued
6 more rapid increase in temperature of the dust – black carbon mixture is thought to be due to
7 the dust.

8



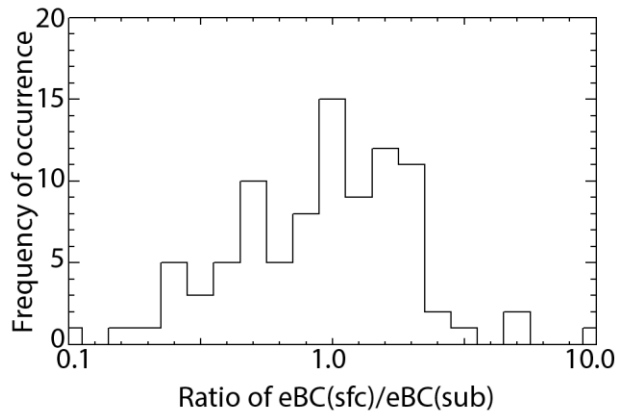
1
2
3
4
5
6
7

Figure 5. Plot showing the relationship between eBC as determined from the LAHM analysis and refractory black carbon as determined by the SP2 instrument ($r^2=0.92$). The values near 0.0 refractory BC are from Pisco mountain in region 2 while the higher values are from Vallunaraju in region 4. The 1 to 1 line is plotted to guide the eye.



1
2
3
4
5

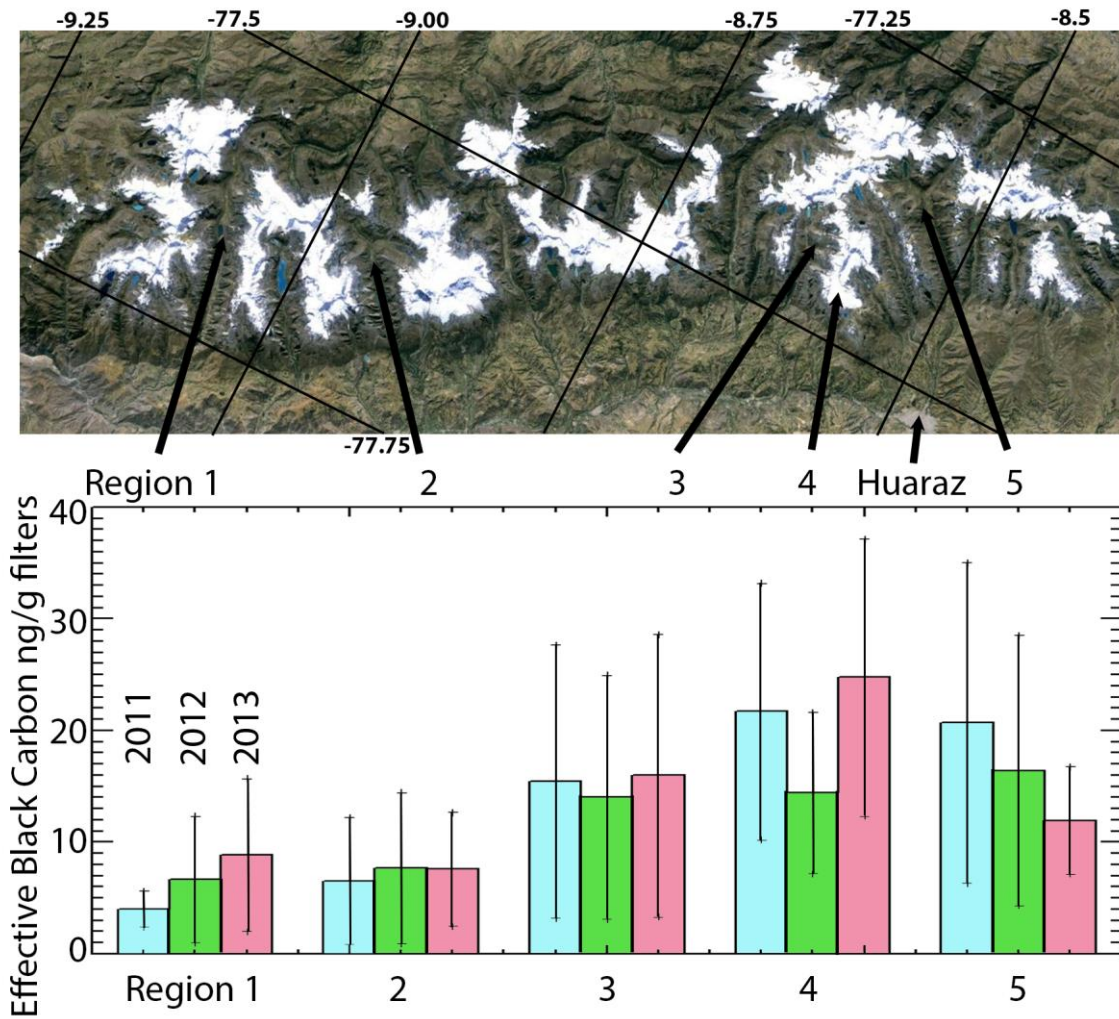
Figure 6. Complete dataset of eBC values determined from the LAHM analysis plotted versus altitude.



1

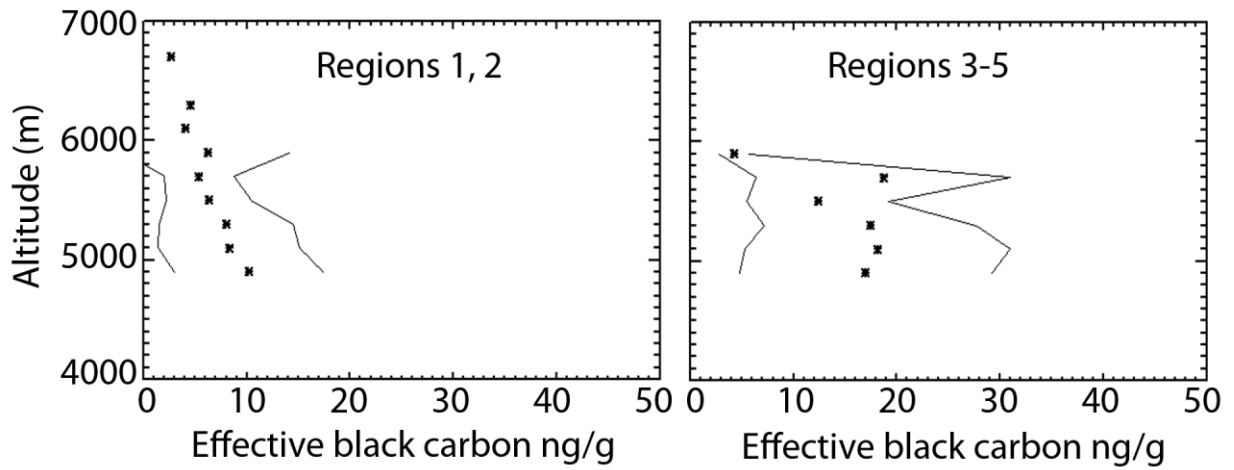
2 Figure 7. Probability distribution function of the ratio of the eBC value measured for surface
 3 samples divided by the eBC value measured for sub-surface samples presented. X-axis is on a
 4 log scale and bins are logarithmically spaced.

5



1
2
3
4
5
6
7
8
9

Figure 8. Google map image of the Cordillera Blanca mountain range. The five regions as well as the city of Huaraz are indicated on the map by black arrows. Average eBC values as determined from the LAHM analysis are shown in the plot for each of the three years. The thin lines indicate \pm one standard deviation of the measurements. Note that in 2013, region 2, SP2 samples averaged 0.65 ng/g rBC indicating that most of the 8 ng/g of the eBC estimate could be due to light absorption by dust.

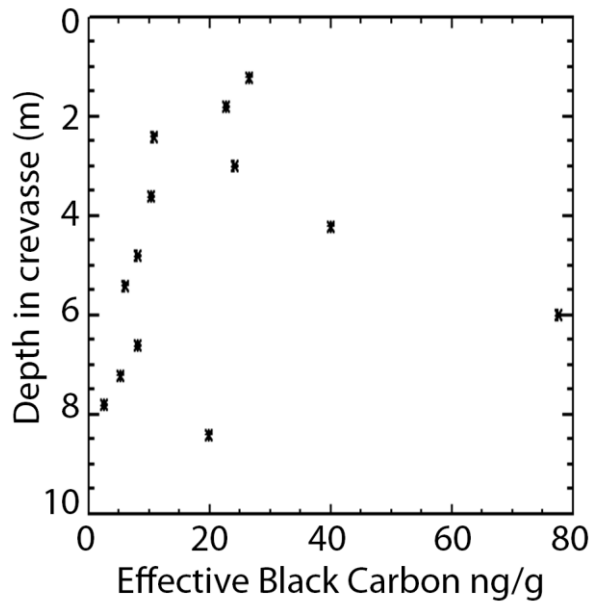


1

2

3 Figure 9. LAHM determined eBC values averaged by altitude bins plotted with ± 1 standard
 4 deviation (lines) by altitude for the Northern (regions 1 and 2) mountains and the Southern
 5 (regions 3-5) mountains in the Cordillera Blanca. Absorbing particles in snow in regions 1
 6 and 2 are likely primarily dust while regions 3-5 are strongly influenced by pollution from the
 7 city of Huaraz.

8



1

2

3 Figure. 10. eBC from snow samples collected from the walls of a crevasse on Vallunaraju
 4 (region 4) the nearest high mountain to Huaraz. A decreasing trend with depth is noted.
 5 These lowest samples were visually the cleanest snow samples from the crevasse walls, and
 6 were likely to have accumulated during the wet season. The points at 4, 6, and 8.5 m were
 7 thin noticeably dark layers.